IOPscience iopscience.iop.org

Home Search Collections Journals About Contact us My IOPscience

Formation of Si/Ge nanostructures at surfaces by self-organization

This article has been downloaded from IOPscience. Please scroll down to see the full text article.

2004 J. Phys.: Condens. Matter 16 S1535

(http://iopscience.iop.org/0953-8984/16/17/006)

View the table of contents for this issue, or go to the journal homepage for more

Download details:
IP Address: 129.252.86.83
The article was downloaded on 27/05/2010 at 14:29

Please note that terms and conditions apply.

INSTITUTE OF PHYSICS PUBLISHING JOURNAL OF PHYSICS: CONDENSED MATTER

J. Phys.: Condens. Matter **16** (2004) S1535–S1551 PII: S0953-8984(04)67191-8

Formation of Si/Ge nanostructures at surfaces by self-organization

Bert Voigtländer, Midori Kawamura, Neelima Paul and Vasily Cherepanov

Institut für Schichten und Grenzflächen (ISG), and cni—Centre of Nanoelectronic Systems for Information Technology, Forschungszentrum Jülich, 52425 Jülich, Germany

Received 1 August 2003
Published 16 April 2004
Online at stacks.iop.org/JPhysCM/16/S1535
DOI: 10.1088/0953-8984/16/17/006

Abstract
The growth of kinetically self-organized 2D islands in Si/Si(111) epitaxy is described. The island size distribution for this system was measured using scanning tunnelling microscopy (STM). The influence of surface reconstructions on growth kinetics is studied directly using a method of simultaneous deposition and STM scanning. For the case of growth of Si islands on Si(111), lateral growth of rows of the width of the 7×7 reconstruction unit cell at the edges of two-dimensional islands leads to the formation of 'magic' island sizes. The evolution of the size and shape of individual {105} faceted Ge islands (hut clusters) on Si(001) is measured during growth. A slower growth rate is observed when an island grows to larger sizes. This behaviour can be explained by kinetically self-limiting growth. The potential formation of thermodynamically stable strained islands of a specific size is discussed. The formation of 2D Si/Ge nanostructures at pre-existing defects is studied. The step flow growth mode is used to fabricate Si and Ge nanowires with a width of 3.5 nm and a thickness of one atomic layer (0.3 nm) by self-assembly. One atomic layer of Bi terminating the surface is used to distinguish between the elements Si and Ge. A difference in apparent height is measured in STM images for Si and Ge. Also different kinds of two-dimensional Si/Ge nanostructure such as alternating Si and Ge nanorings having a width of 5–10 nm were grown.

(Some figures in this article are in colour only in the electronic version)

1. Introduction

Several approaches are used for fabricating nanostructures at surfaces. Relatively large structures are created by lithography. The greatest advantage of lithographic patterning is the very large variety of different structures which can be defined by lithographic methods. On the other hand lithographically defined structures are usually quite large nanostructures.

The resolution of optical lithography is approaching ~100 nm while the resolution of electron beam lithography reaches even smaller dimensions. However, since writing with electron beam lithography is a sequential method it is not possible to fill a whole wafer with small structures in a reasonable time. Due to the limitations of the lithographic methods to fabricate nanostructures, new approaches are explored for the formation of smaller nanostructures. The most extreme approach is to build nanostructures 'bottom up' atom by atom with the help of a scanning tunnelling microscope at low temperatures [1]. This approach is the ultimate in terms of the size of a nanostructure. Of course this is a very slow method for building nanostructures. Usually a couple of hours are required to write some characters.

An alternative approach for the formation of small nanostructures is self-organization of atoms. Here four different kinds of self-organization of nanostructures at surfaces are considered. First the formation of kinetically self-organized nanostructures formed during molecular beam epitaxy will be discussed. The island structures formed by kinetic self-organization can be quite small; however, the size uniformity is a challenge. A second topic will be to show approaches for the formation of thermodynamically (meta)stable nanostructures. Here the size uniformity should be best. A third approach is the ordered formation of nanostructures by nucleation of islands at defect sites which pre-exist at (or below) the surface. These defect sites can be for instance dislocations or step bunches. As a fourth method, promising approaches of combination of self-organization with lithography methods, so-called 'hybrid methods', are discussed.

2. Kinetically self-organized islands

During molecular beam epitaxy (MBE) growth of silicon, atoms deposited onto the surface diffuse on the surface and can be incorporated into pre-existing step edges if the diffusion length is sufficient (figure 1). When the diffusion is slower, diffusing atoms will meet and an island will nucleate on the surface. The island will grow further by attachment of diffusing atoms at the island [2] (figure 1). The islands which form after deposition of less than an atomic layer (monolayer ML) of Si are called 2D islands, because their thickness is only one (or two) atomic layers. The islands grow epitaxially which means that they arrange in a crystalline structure in registry with the underlying substrate atomic structure. The shape of the islands depends on the atomic structure of the underlying substrate surface. For the case of Si(111) as substrate the substrate crystal structure has a threefold rotational symmetry at the surface. Therefore the 2D Si islands on Si(111) have triangular shape (figure 2).

Two-dimensional islands are the simplest example showing self-organized growth of nanostructures. In the following it will be shown how the density and the size of these islands can be controlled by the kinetic parameters temperature and growth rate. First, the deposition temperature influences the island density strongly as shown by the comparison of figures 2(a) and (b). When the island density is plotted as function of temperature (figure 3(a)) it can be seen that the island density follows an Arrhenius law: $n \sim \exp(E_{\mathrm{act}}/kT)$, with E_{act} being an effective activation energy consisting of a diffusion energy and binding energy component. The temperature is one important parameter of growth kinetics, the deposition rate is another. It is found that the island density scales with the deposition rate in the form of a power law $n \sim F^{\omega}$ with a scaling exponent ω. From figure 3(b) the scaling exponent is determined as $\omega = 0.75$ for Si/Si(111) homoepitaxy. Combining the temperature and the rate dependence results in the following scaling law: $n \sim F^{\omega} \exp(E_{\mathrm{act}}/kT)$ [4]. This shows that the island density can be controlled over a wide range by adjusting the kinetic growth parameters temperature and growth rate. The average island distance is just the square root of the inverse of the island density $L = 1/\sqrt{n}$.

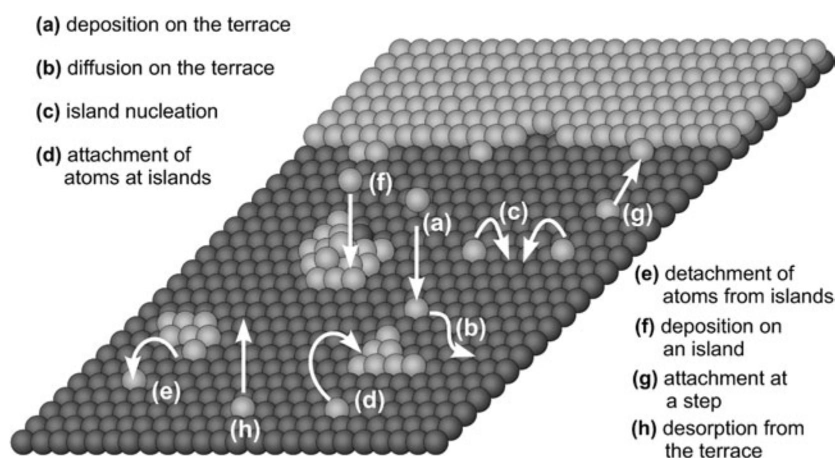

Figure 1. Schematic representation of different fundamental processes occurring during epitaxial growth leading to self-organization of two-dimensional islands.

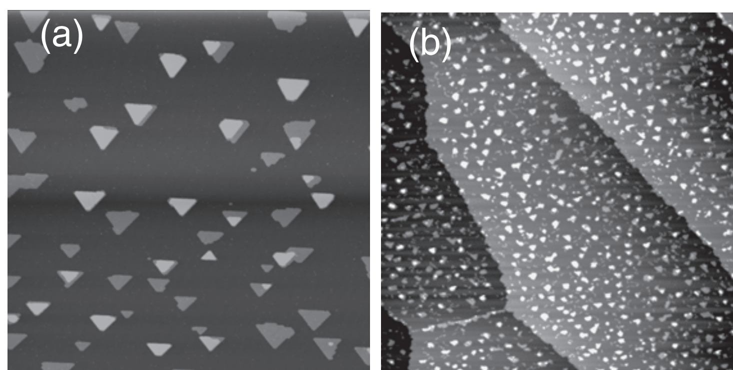

Figure 2. Scanning tunnelling microscope images after the growth of 0.2 atomic layers of silicon on a Si(111) surface. The islands have triangular shape due to the symmetry of the substrate and have a height of one atomic layer (dark grey) or two atomic layers (light grey). The island density depends on temperature, as can bee seen is seen by comparison of growth at the high temperature of 770 K (a) to growth at a lower temperature 610 K (b). Both images have a size of 350 nm.

The nucleation of the islands is a random process. Despite this the distribution of the island sizes has a peak (figure 4). This arises due to a saturation of the island nucleation as will be explained in the following. In the early stage of growth islands nucleate randomly on the surface and the distance between the islands decreases. If the distance between the islands is equal to the mean distance which an adatom travels before a nucleation event happens, then the incorporation of adatoms in existing islands becomes a more probable event than the nucleation of new islands. Around each island a 'capture zone' exists. Adatoms deposited in this capture zone attach to the corresponding island. Without this effect the distribution of island sizes would be even broader. The nucleation of further islands is suppressed beyond a certain coverage. The effect of the capture zone gives rise to two regimes in the island growth: the very early regime (nucleation regime) is characterized by the nucleation of islands (<0.1 ML deposited). In the second regime the capture zones of existing islands overlap and

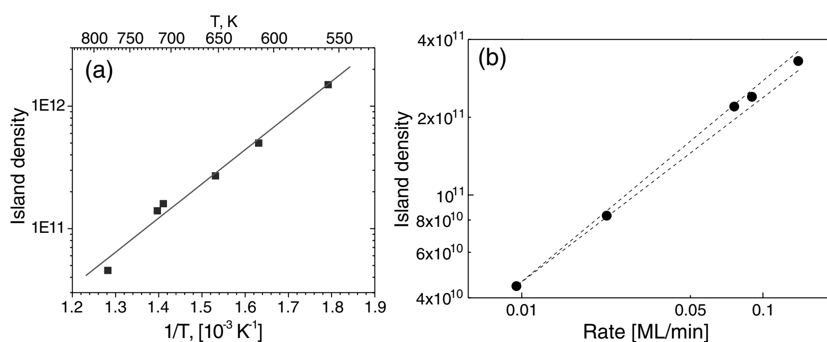

Figure 3. The island density shows an Arrhenius behaviour as function of temperature (a). As a function of deposition rate a power law is found for the island density (b) [3]. This shows that the island density can be controlled by the kinetic parameters temperature and deposition rate. The island density is given in cm^{-2}.

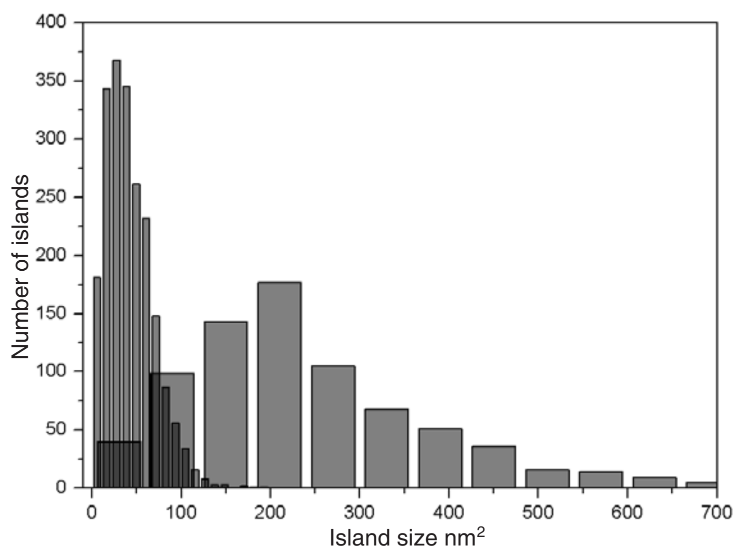

Figure 4. Island size distribution for two-dimensional Si islands on Si(111). The width of the distribution is of the order of the average size of the islands. Two distributions for two different temperatures are displayed. The narrow bins (peak at small island sizes) correspond to deposition at 610 K. The distribution with the wide bins (peak at larger island sizes) corresponds to deposition at 710 K.

the nucleation of new islands ceases. This regime is characterized by growth of existing islands to a larger size and is called the growth regime. The average island size can be controlled by the deposited amount. The island size distributions for two different temperatures are shown in figure 4. It is seen that the peak in the island size distribution scales towards larger sizes with larger temperatures.

In summary, the island density of two-dimensional islands can be controlled by the kinetic parameters temperature and deposition rate, while the size distribution is quite broad due to the stochastic nature of the nucleation of the islands.

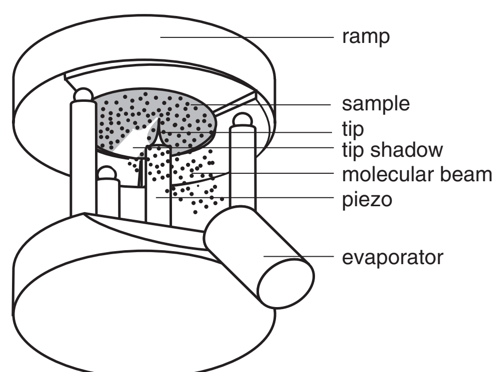

Figure 5. The principle of the STM design which is used for simultaneous STM scanning and MBE growth at high temperatures.

3. Fundamental processes in Si/Si and Ge/Si epitaxy studied by scanning tunnelling microscopy during growth

Here a mode of STM operation is described which opens the possibility of observing the dynamics during epitaxial growth '*in vivo*' (MBSTM). The experiments were performed in a standard ultrahigh vacuum system. Due to the open design of the STM the molecular beam from an evaporator can be directed towards the sample while the STM is scanning the surface (figure 5) [2, 5, 6]. During imaging the sample is held at MBE growth temperatures of 600–900 K. Continuous imaging of the growing surface results in movies showing details of the growth process on the atomic level. Some of the movies can be accessed on the Internet: http://www.fz-juelich.de/isg/voigtlaender.

3.1. Influence of the (7 × 7) reconstruction in Si/Si(111) epitaxy

During the epitaxial growth of 2D Si islands on Si(111) the growth of a selected island can be observed as a function of time. The two-dimensional triangular islands that form during submonolayer growth of Si on Si(111) are 1 BL high (1 BL = one (111) bilayer = 3.1 Å = 2 ML). Figures 6(a)–(f) show STM images from a growth sequence of such an island. In (a), the shape of the island is triangular. Images (b)–(d) show the same island at a later stage during growth. As shown by images (b)–(d), growth proceeds by advancement of a row of a certain width along the right island edge. The position of the kink at which the row is ending is shown by an arrow in (b)–(d). An analysis of the width of this row and further atomically resolved images show that the width of such a row is 27 Å, which is just the width of one 7 × 7 reconstruction unit cell [7].

In the following the influence of the 7 × 7 reconstruction on the growth behaviour will be discussed. The rhombic unit cell of this reconstruction consists of two triangles. One of these triangles has a stacking fault in the surface layers, relative to the substrate stacking (F-HUC). The other triangle of the reconstruction unit cell is unfaulted relative to the substrate (U-HUC); figure 7(a).

During lateral growth of an island, the surface reconstruction of the substrate has to be lifted and the substrate atoms have to rearrange to the bulk structure. This transformation of the reconstructed surface layer towards the bulk structure is a general phenomenon which has to occur in any epitaxial growth at reconstructed surfaces. It requires a higher energy to lift the

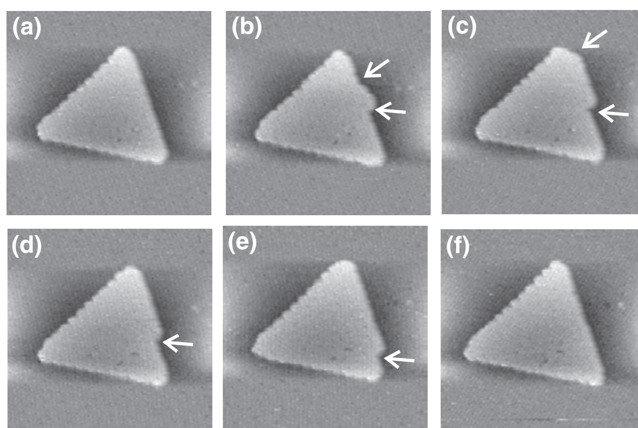

Figure 6. A sequence of images showing the lateral growth of a triangular Si(111) island. A row of the width of the 7×7 unit cell is growing along the right edge of the island (b)–(f). The image size is 500×500 Å^2, $T = 575$ K. The complete growth sequence is available as a movie on the World Wide Web: http://www.fz-juelich.de/video/voigtlaender.

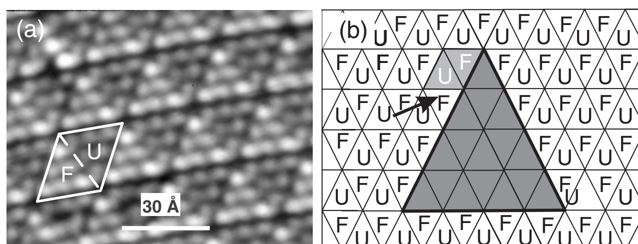

Figure 7. (a) An STM image of the Si(111)-7×7 reconstruction. The white protrusions are the Si adatoms. The unit cell is indicated by a white rhombus. A dashed line divides two triangular subunits. Since the image is taken at negative sample bias (-2 V), the adatoms in the faulted half of the unit cell (F) appear brighter than those in the unfaulted half (U). (b) The arrangement of the U and F parts of the 7×7 unit cell on the substrate around a triangular island (shown in grey).

reconstruction of the F-triangle as compared to the U-triangle [8]. To lift the reconstruction in the U-triangle, only atoms in the uppermost adatom layer have to rearrange. This is associated with a relatively low energy barrier. Lifting the reconstruction of the F-triangle requires the removal of the stacking fault in the layer below the adatoms. This rearrangement of atoms in deeper layers is associated with a larger energy barrier. This should lead to a high activation barrier for overgrowth of the F-triangle compared to overgrowth of the U-triangle.

In figure 7(b), a Si island (grey) and the U and F triangles of HUC of the surrounding reconstructed substrate surface are shown. Due to the crystallographic orientation of the island, it is surrounded only by substrate F-HUC. This means that further lateral growth (initiated by the overgrowth of an F-triangle) is hindered by a high energy barrier. Once an F-triangle has nucleated, the neighbouring U-triangles can be overgrown more easily (no stacking fault has to be removed). The overgrowth of the next F-triangle is facilitated by the existence of a 'macro-kink' (arrow in figure 7(b)). Here the cost of the stacking fault energy is reduced by a gain in the island edge energy: the edge length is reduced after growth of an F-triangle. Therefore, neighbouring U and F units can be overgrown in quick succession, leading to the fast growth of a stripe of the width of the 7×7 unit cell.

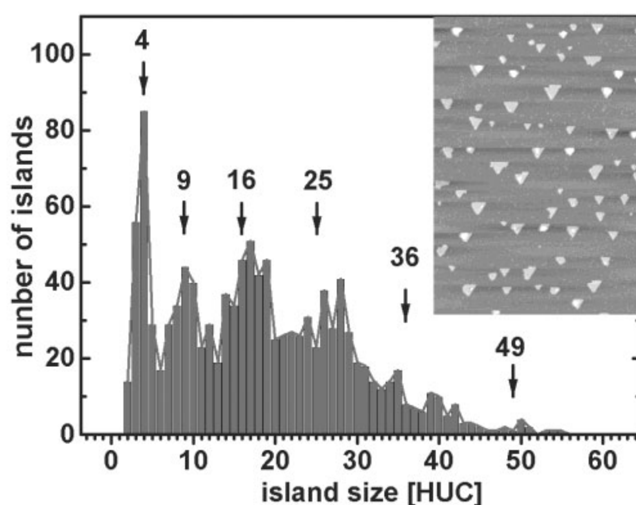

Figure 8. The experimentally observed island size distribution with peaks at the 'magic' sizes of 4, 9, 16, 25, . . . half unit cells (HUC). These islands have closed shells corresponding to stable island sizes. A STM sample image of 2D islands is shown in the inset (2000 × 3000). 7% of a bilayer of Si was deposited at a sample temperature of 725 K and a deposition rate of 0.5 BL min^{-1}.

Due to the quick growth of a row once it is nucleated and a longer time until the nucleation of the next row the island shape of a completed triangle is found often in snapshot images of the island morphology. Islands of complete triangular shape are kinetically stabilized. This higher stability for the closed shell triangular islands leads to pronounced peaks of islands of 'magic' sizes in the measured island size distributions [9]. Peaks in the island size distribution are observed for the stable island sizes: 4, 9, 16, 25, . . . half unit cells (HUC) for which closed shell triangular islands occur (figure 8).

In the following the competition between kinetics and thermodynamics with respect to the shape of 2D islands will be demonstrated. The shape of the islands depends not only on the atomic structure of the underlying substrate but at high temperatures an equilibrium island shape forms. It will be shown that a *kinetically* limited growth shape occurs during growth, while equilibration of these islands without an external flux results in a transition to the hexagonal equilibrium form.

In figure 9 two islands are imaged first during growth (figure 9(a)), then after a growth interruption of 18 min (figure 9(b)), and finally after the growth was resumed (figure 9(c)) [2]. These experiments show that when growth is interrupted, the islands quickly lose their triangular shapes. First, the atoms from the apex regions detach creating islands with rounded corners. Subsequently, the island shapes turn more slowly into a hexagon-like (compact) shape as shown in figure 9(b). When growth is continued, the islands quickly resume triangular shapes again. This evolution of growth morphology from triangular islands during evaporation to hexagonal islands upon equilibration of the surface at 725 K and the final transition back to triangular islands when the external flux is resumed and the equilibrium conditions are no longer maintained are clearly shown in figure 9. This process shows that the triangular island shapes are non-equilibrium ones while equilibrium shapes are close to hexagons.

The equilibrium shape of an island is the form for which the energy of the island is minimized. If the steps in the $[\bar{1}\bar{1}2]$ and the $[11\bar{2}]$ direction were equivalent, the equilibrium shape would be an equilateral hexagon. During annealing the form of the islands approaches

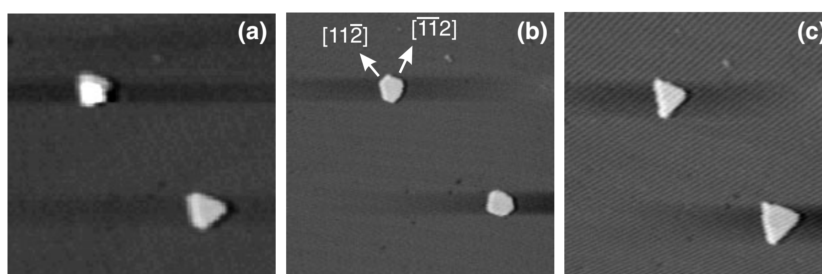

Figure 9. Evolution of island shapes during growth and growth interruption (at a substrate temperature of 725 K). Imaged during growth, islands have a triangular form (a). After 18 min of annealing at 775 K, the islands have changed their shape to hexagonal (rounded) (b). After growth commenced again, the island shapes changed back to triangular (c). In all three images, snapshots of the same two islands are shown. The image size is 550 × 550 Å^2.

such a hexagon. However several observations after long times of annealing show that the edges perpendicular to [11$\bar{2}$] are a bit shorter than the edges perpendicular to the [$\bar{1}\bar{1}$2] direction. This indicates that the edges perpendicular to [11$\bar{2}$] have a higher energy.

3.2. Kinetically self-limiting growth of Ge islands on Si(001)

In Ge epitaxy on Si(001) three-dimensional Ge, islands with {105} facets nucleate after the completion of the 2D wetting layer [10]. The island edges are oriented along ⟨100⟩ directions, i.e. at 45° to the direction of the reconstruction dimer rows. The strain of these islands is partially relaxed elastically, but they are coherent with the substrate lattice (i.e., free of dislocations between the substrate and the hut clusters) [10]. The evolution of the growth of these hut clusters is observed by STM during growth. A sequence of STM images for increasing coverage is shown in figure 10. From the images for instance the volume of the hut clusters can be calculated.

Figure 11 shows the evolution of the volume of several individual islands as a function of total deposited coverage. The initially higher growth rate of individual islands just after the nucleation, indicated by initially large slopes in figure 11, decreases when the islands grow to a larger size. In the following, a model is used which shows that kinetically self-limiting growth explains the observed slower growth for larger island sizes. This kinetic model for the growth of hut clusters relies on a barrier to the nucleation of each successive atomic layer on the {105} facets [11, 12]. The barrier to the nucleation of a new facet increases with the facet size. This size dependent nucleation barrier for the repeated overgrowth of the {105} facets is the reason for the self-limiting growth behaviour [12]. Results of the model calculations for the evolution of the hut cluster volume are shown as solid and dashed lines in figure 11 and are in good agreement with the experimental data. The experimentally observed slower growth rate for larger islands is clearly reproduced. This indicates that a kinetic self-limitation is effective during the growth of larger hut clusters. This kinetic self-limitation arises due to an energy barrier for the nucleation of new material on completely filled {105} facets.

4. Thermodynamically stable nanostructures

If nanostructure islands were thermodynamically stable their size distribution could be narrow. A thermodynamically stable island size means that the energy (per atom) has a minimum for this stable size. For configurations with larger or smaller islands the energy (per atom) would be

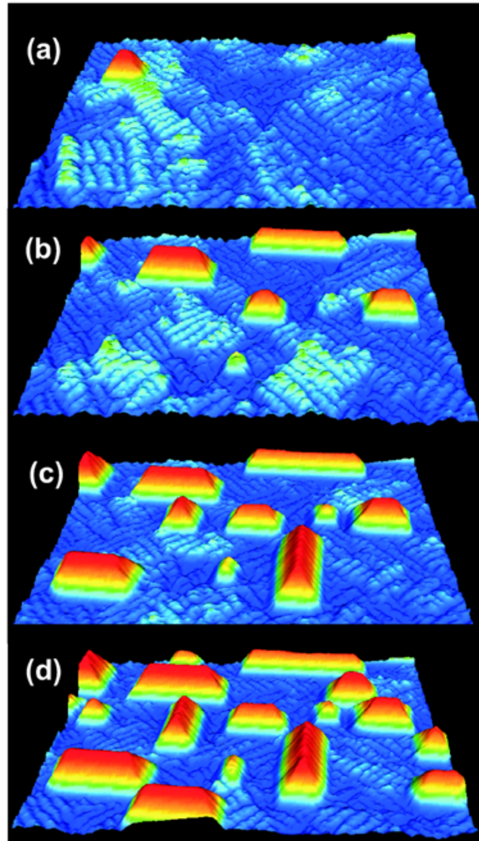

Figure 10. Perspective views of STM sample images of the hut cluster growth as function of coverage beyond the wetting layer. (0.07, 0.46, 1.33 and 1.81 ML from the top to the bottom; image area: 1300×1000 Å^2, $T = 575$ K). The complete growth sequence is available as a movie on the World Wide Web: http://www.fz-juelich.de/video/voigtlaender/.

higher. Therefore one has just to approach thermodynamic equilibrium to obtain a very narrow island size distribution. One way to achieve thermodynamic equilibrium is to heat a sample with different island sizes present and wait until equilibrium has established. The equilibrium configuration will be established by material transport between the islands. Atoms will detach from islands with higher energy and attach to islands with a lower energy (per atom).

To describe material transport in a system with a variable number of atoms the chemical potential is used. The chemical potential is the change of the energy (of an island) when the number of particles changes, $\mu = \mathrm{d}E/\mathrm{d}N$. During equilibration, atoms detach from islands where the chemical potential is highest and attach to islands with a lower chemical potential. This lowers the total energy of the system. Therefore the material transport between different islands is governed by the chemical potential. A simple example is the chemical potential of quadratic 2D islands of dimension L (figure 12(a)). The energy difference between different sized islands comes from the edge energy (β is the edge energy per length). The energy of an island is $E = E_{\mathrm{edge}} = 4L\beta$. The number of atoms in an island (N) depends on the dimension L as $N = L^2/\Omega$ with Ω being the area per atom. The chemical potential is

$$\mu = \frac{\mathrm{d}E}{\mathrm{d}N} = \frac{2\Omega\beta}{L} \sim \frac{1}{L}. \tag{1}$$

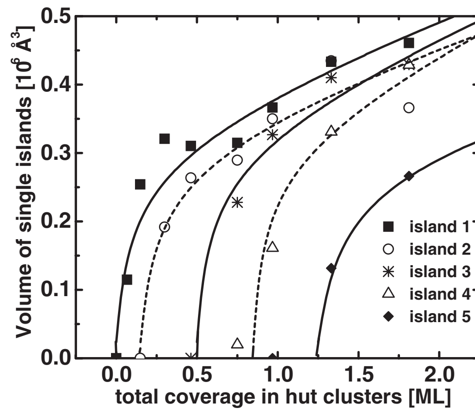

Figure 11. Evolution of the volume of individual hut clusters. The different symbols correspond to different individual islands. The size evolution shows self-limiting behaviour: the initially larger growth rate (large slope) just after the nucleation decreases when the islands grow larger. Results of a model calculation of kinetically self-limiting growth including a kinetic energy barrier for the nucleation of new material on the facets are shown as solid and dashed curves.

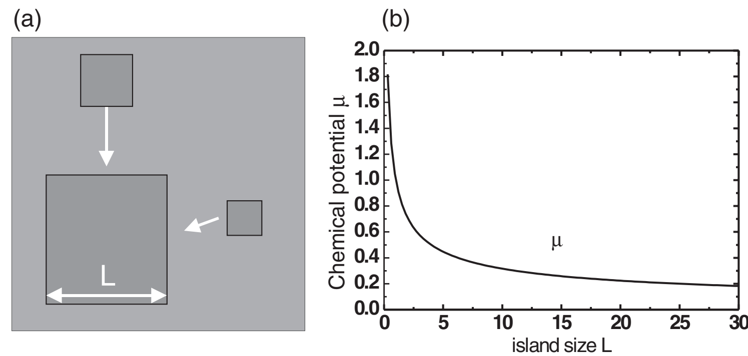

Figure 12. (a) Coarsening of a large island at the expense of small ones. (b) The chemical potential of an island.

Since μ is decreasing for larger islands (figure 12(b)), infinite size islands have the lowest chemical potential. This means that the stable island is infinitely large. In this case the equilibration does not result in a stable finite island size. Equilibration in this model by material transport between islands is also called coarsening because it results in the shrinkage of small islands and growth (coarsening) of large islands.

An infinitely large stable island size is the result for homoepitaxial growth, taking into account only the step energy. The situation becomes different when elastic stress is also taken into account as it occurs in heteroepitaxy [14]. Here stress is induced by the different lattice constants of the substrate material and the material of the islands. The elastic effect of strained two-dimensional islands can be approximated by that of a surface stress domain; i.e. the surface stress at the area of the island is different from that at the rest of the surface (figure 12). The strain energy of a quadratic surface stress domain can be calculated using the elastic theory as $E_{\text{strain}} = 2LC' \ln L$ [13]. Adding the step edge energy results in a total energy of a strained island:

$$E = E_{\text{edge}} + E_{\text{strain}} = 2L[2\beta - C' \ln L]. \tag{2}$$

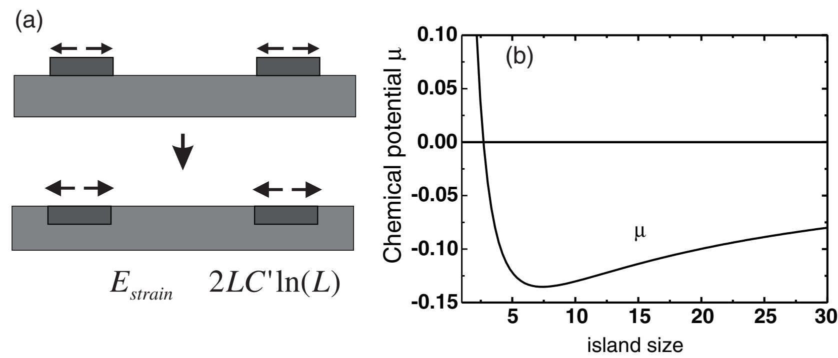

Figure 13. (a) The elastic stress induced by two-dimensional islands with a different lattice constant to the substrate can be approximated by surface stress domains. (b) The chemical potential of an island with a energy component due to elastic strain being included.

This results in a chemical potential

$$\mu = \Omega\left[\frac{2\beta - C'}{L} - \frac{C'}{L}\ln L\right] \tag{3}$$

which is plotted in figure 13. In this case the chemical potential has a minimum at the size $L_{\min} = \exp(2\beta/C')$. This would mean that during coarsening the islands would approach this size. Larger islands would dissolve and smaller islands grow until all islands have size $L_{\min}$, i.e. the lowest chemical potential. This would result in a very narrow size distribution. Unfortunately step energies are only very poorly known, so it is not possible to predict a reliable number for the equilibrium island size. An experimental realization of a thermodynamically stable islands has not yet been confirmed.

The most perfect thermodynamically stable nanostructures are surface reconstructions with a relatively large unit cell. The atomic arrangement at surfaces, especially at semiconductor surfaces, often deviates strongly from the atomic structure expected for a bulk terminated surface obtained when the atomic arrangement of the surface atoms remains like the bulk structure [2]. The atoms at the surface rearrange (reconstruct) in order to reduce the number of unsaturated bonds (dangling bonds) at the surface. The most famous surface reconstruction with a large unit cell is that of the Si(111)-(7 × 7) surface shown in figure 7(a). The length of the triangular subunits is 2.7 nm. These are very small nanostructures because the main driving force for the formation of these structures is the minimization of the energy of the covalent bonds at the surface. Covalent bonding is a short range interaction compared to elastic interactions considered above. Another example of a surface reconstruction with a large periodicity is a 3 ML thick Ge layer terminated with Sb [15]. This layer forms a hexagonal arrangement with a period of 4 nm (figure 14). Here both covalent bonding and the misfit strain induced by the larger lattice constant of the Ge are important for the formation of the hexagonal nanostructures.

In the following the formation of nanostructures in equilibrium is compared to the formation of nanostructures by growth kinetics. Equilibrium nanostructures have the advantage of a narrow size distribution around the optimum size. A disadvantage is that the size is determined by the material parameters (strain energy and step edge energy for instance) and cannot be tuned independently. The size and density of nanostructures formed under kinetic conditions can be tuned easily by variation of the growth parameters. On the other hand the size uniformity of the islands is relatively poor.

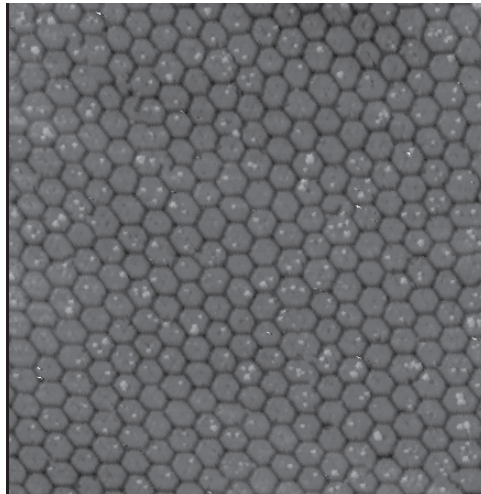

Figure 14. Hexagonal surface reconstruction on a Sb/Ge/Si(111) surface (periodicity 4 nm). Surface reconstructions are the most regular nanostructures at surfaces.

5. Lateral positioning of islands

In the examples considered up to now the positions at which the nanostructured islands formed were not predictable due to the stochastic nature of the nucleation process. It is desirable to position islands at specific (preselected) locations. This is desirable if the islands will be used as functional units of nanoelectronic devices. Electric contacts can be structured more easily when the location of an island is predefined. In this section approaches will be discussed where island nucleation occurs not randomly, but at specific locations. These predefined locations are usually defect sites on regularly prestructured substrates. Examples of such prestructured substrates are: regularly stepped substrates, faceted substrates, a regular arrangement of dislocations, or long range surface reconstructions.

An example of ordered nucleation at a prestructured substrate is shown in figure 15(a). Here Ge islands nucleate above dislocation lines. A SiGe film is grown on a Si(001) substrate. At the interface between the SiGe film and the substrate, dislocations form. The driving force for the formation of the dislocations is the relief of elastic strain which arises due to the different lattice constants of the Si substrate and a Ge/Si film on this substrate. Due to the crystal structure of the substrate the dislocations are aligned in straight lines along the two perpendicular high symmetry directions of the substrate. During annealing the dislocations form a relatively regular network, due to a repulsive elastic interaction between the dislocations. Figure 15(a) shows growth of Ge islands on this prestructured substrate [17]. Rows of islands grow preferentially above the dislocation lines. This preferred nucleation at the dislocation lines can be explained as follows. A GeSi alloy has a natural lattice constant which is larger than that of the Si substrate. However, a thin Ge/Si film epitaxially grown on a Si substrate is confined to the lattice constant of the substrate. Therefore, the GeSi film is compressively strained and this compressive strain is locally relaxed above the strain relieving misfit dislocations. The areas above the dislocations have a larger lattice constant (close to the natural lattice constant of the GeSi alloy) while the areas far from the dislocations are compressively strained. The nucleation of Ge islands is more favourable at the relaxed areas above the dislocations which have a lattice constant closer to that of Ge than the strained areas of the SiGe film where the lattice constant

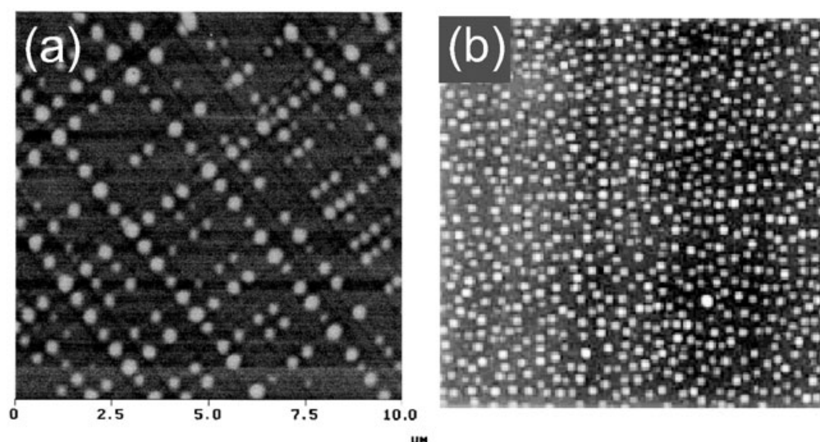

Figure 15. (a) Ordered nucleation of Ge islands which is prestructured by an underlying network of dislocations. (b) Germanium islands grown on a substrate without dislocations for comparison [17]. Image sizes 7 μm.

is confined to being that of the Si substrate. Islands have a lower energy if they grow with their natural lattice constant compared to growth at a different lattice constant (strained islands). This leads to a preferred nucleation of Ge islands above the dislocations. The nucleation does not occur randomly at the surface, but nucleation occurs simultaneously at sites which have the same structure. This leads to a narrower size distribution than for the growth on unstructured Si(001) substrates (figure 15(b)).

In the case of the growth on a patterned substrate another process of self-organization occurs (before the growth of islands) during the formation of the regular arrangement of the defect structures. Here it is often a repulsive elastic interaction which leads to a regular distance between steps or dislocations under equilibrium conditions. Since island nucleation occurs at the defect sites, the distances are determined by the distances of the defects. Nucleation at predefined defect sites has two advantages over the random nucleation. First the islands are located at specific sites and second the size distribution is narrower due to simultaneous nucleation at sites with identical environments.

6. Formation of nanowires at the atomic scale

Up to now several approaches for the self-organized growth of islands have been discussed. Here, results on the formation of nanowires are summarized. One approach for the synthesis of epitaxial nanowires at surfaces is to use pre-existing step edges on the Si(111) surface as templates for the growth of two-dimensional Ge wires at the step edges. When the diffusion of the deposited atoms is sufficient to reach the step edges, these deposited atoms are incorporated exclusively at the step edges and the growth proceeds by a homogeneous advancement of the steps (step flow growth mode) [2]. If small amounts of Ge are deposited the steps advance only some nanometres and narrow Ge wires can be grown. A key issue for the controlled fabrication of nanostructures consisting of different materials is a method of characterization which can distinguish between the different materials on the nanoscale. In the case of the important system Si/Ge it has been difficult to differentiate between Si and Ge due to their similar electronic structures. However, if the surface is terminated with a monolayer of Bi it is possible to distinguish between Si and Ge. Figure 16(a) shows an STM image after repeated

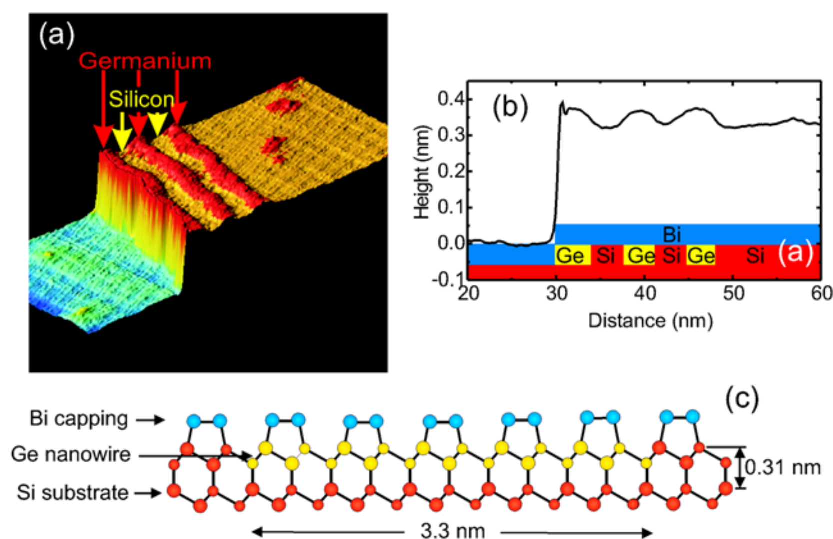

Figure 16. (a) An STM image of two-dimensional Ge/Si nanowires grown by step flow at a pre-existing step edge on a Si(111) substrate. Si wires (light) and Ge wires (dark) can be distinguished by the different apparent heights. (b) The cross section along the white line in (a) shows the dimensions of the Si and Ge nanowires. The width of the wires is 3.5 nm and the height is only one atomic layer (0.3 nm). (c) The atomic structure of a 3.3 nm wide Ge wire on the Si substrate capped by Bi. The cross section of the Ge wire contains only 21 Ge atoms [16].

alternating deposition of 0.15 atomic layers of Ge and Si. Due to the step flow growth, Ge and Si wires are formed at the advancing step edge. The elements can be easily distinguished by the apparent heights in the STM images. It turned out that the height measured by the STM is higher on areas consisting of Ge (dark stripes) than on areas consisting of Si (light stripes). The assignment of Ge and Si wires is evident from the order of the deposited materials (Ge, Si Ge, Si and Ge, respectively, in this case). The initial step position is indicated by white arrows in the right part of figure 16(a). The step edge has advanced towards the left (arrowheads in figure 16(a)) after the growth of the nanowires. The reason for the STM height difference between Si and Ge is the different electronic structure of a Ge–Bi bond compared to a Si–Bi bond. The apparent height of Ge areas is ∼0.1 nm higher than the apparent height of Si wires (figure 16(b)). The width of the Si and Ge wires is ∼3.5 nm as measured from the cross section (figure 16(b)). The nanowires are two dimensional with a height of only one atomic layer (∼0.3 nm). Therefore, the cross section of a 3.3 nm wide Ge nanowire contains only 21 atoms (figure 16(c)). The height difference arises due to an atomic layer of Bi which was deposited initially. The Bi always floats on top of the growing layer because it is less strongly bound to the substrate than Si or Ge. The Si/Ge wires are homogeneous in width over larger distances and have a length of several thousand nanometres. Different widths of the wires can be easily achieved by depositing different amounts of Ge and Si.

7. Formation of more complex nanostructures by self-organization

One disadvantage of the use of self-organization for the formation of nanostructures is that only very simple kinds of nanostructures can be build by self-organization. The only examples presented so far are various kinds of islands and nanowires. In the following it will be shown that, using two-dimensional island growth, a little bit more complex Si/Ge nanostructures,

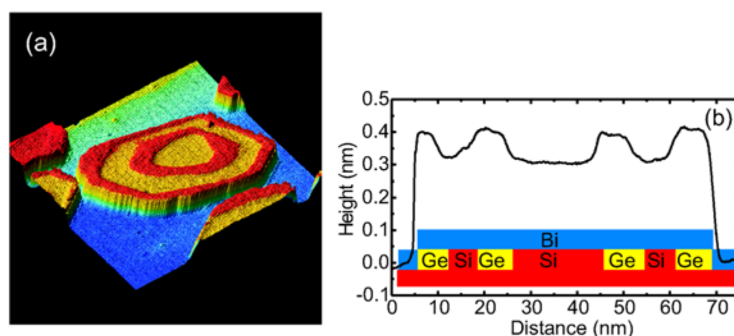

Figure 17. (a) Two-dimensional Ge/Si ring structure imaged with the STM. Ge rings are shown as dark and Si rings are shown as light. The width of the rings is 5–10 nm and the height is one atomic layer (0.3 nm). (b) A cross section across the ring. Due to the Bi termination the Ge rings are imaged 0.09 nm higher than the Si rings. A schematic diagram of the ring structure is shown in the inset [16].

namely Si/Ge ring structures, can be grown by self-assembly (figure 17(a)). In the two-dimensional island growth mode the diffusion of deposited atoms at the surface is reduced (by decreasing the temperature) so most of the diffusing atoms do not reach the step edges but nucleate as two-dimensional islands or attach to existing islands. Once atomic layer high islands have nucleated, deposited atoms diffuse towards the island edge and are incorporated forming a new ring of Ge or Si (figure 17(a)). The measured height of the Ge rings is 0.09 nm higher than the measured height of the Si rings (figure 17(b)). The width of the rings is 5–10 nm and the thickness is only one atomic layer (0.3 nm). The Si/Ge ring structure shown in figure 17(a) was obtained as follows. Initially Si islands form the cores (diameter 10–20 nm) of the Si/Ge ring structures. Subsequent alternating deposition of Ge and Si results in the formation of the Si/Ge ring structures around the Si core.

8. Hybrid methods

In hybrid methods self-organization is combined with lithographic patterning. In this approach self-organization is used to form nanostructures on a smaller scale than the one accessible by lithography. Most importantly the hybrid methods provide direct contact of nanostructures formed by self-organization to mesoscopic lithographically patterned structures. The self-organized growth of Ge islands in oxide holes is shown in figures 18(a)–(d). The starting surface is a silicon substrate with a thin oxide layer at the surface. Electron lithography is used to remove the oxide and form holes of a diameter of 0.5 μm where the bare Si surface is exposed [18]. Self organized growth of Ge leads to the formation of Ge islands which can be smaller than the size scale of the electron beam lithography. The gas phase growth of Ge is selective, i.e. Ge is only growing inside the holes in the oxide and not on the oxide itself. Figure 18 shows the nucleation of Ge islands in the holes in the oxide for different growth temperatures. At lower temperatures the island density is so large that several islands nucleate in one oxide hole. If the temperature is increased, finally only one Ge island nucleates in each oxide hole. The size of the Ge island is smaller than the lithographically defined oxide hole. This approach is called lithographic downscaling. However, the positioning of the islands is not perfect. As seen in figure 18(d) the position of the Ge island inside the oxide hole is not defined but rather randomly in the centre or at the corner of the oxide hole. Due to the fact that the Ge does not grow at the oxide, the edges of the oxide hole are not sinks for deposited Ge atoms. Therefore, the Ge adatom concentration is homogeneous across the hole and the

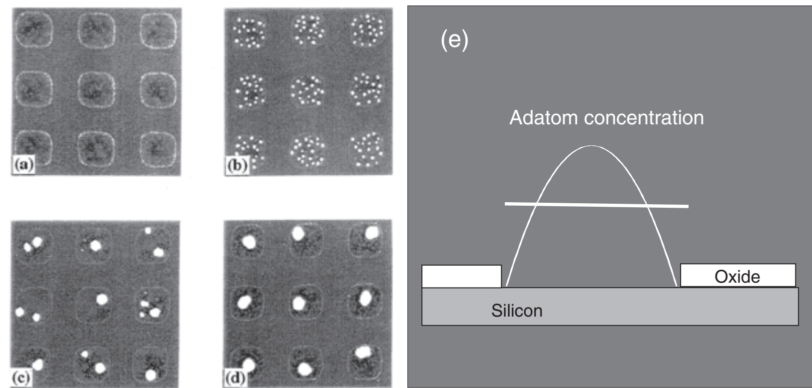

Figure 18. (a)–(d) Growth of Ge islands in holes on an oxidized Si substrate [18]. (e) Adatom density in an oxide hole for the case where the hole edges are sinks of adatoms (parabolic curve) or for the case where the edges are not sinks for adatoms (horizontal line).

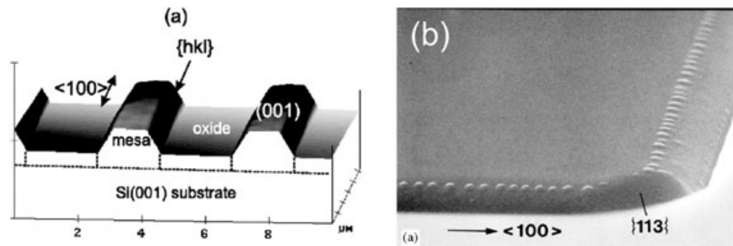

Figure 19. (a) Si mesa structures (width 1 μm) formed by optical lithography. (b) Regular alignment of Ge islands at the mesa edges [19].

nucleation of the Ge island is random within the oxide hole. If the edges of the hole were sinks for Ge atoms (for instance if the edges of the hole consisted of Si) the adatom density would have a maximum at the centre of the hole and the nucleation of Ge islands would occur preferentially at the centre of the oxide holes (18(e)).

A simple structure formed by lithographic methods is a mesa (from the Spanish word for table) which is a flat terrace separated from the rest of the wafer by trenches. A silicon mesa structure is imaged by electron microscopy and shown in figure 19(a). It has been observed that the growth of Ge on this mesa leads to preferential nucleation of Ge islands at the mesa edges [19]. Figure 19 shows a regular alignment of Ge islands along the mesa edges. This preferred nucleation of islands occurs due to a high density of steps at the mesa edges which form sites of preferential nucleation.

Finally, an example is shown where a hybrid method is used to form cobalt silicide nanowires on Si substrates. The complete process involves several steps and is described in [20]. Multiple etching and oxidation steps lead finally to the formation of a silicide wire. The starting point is a $CoSi_2$ layer on a silicon substrate which is pushed locally into the substrate by oxidation. This leads to formation of a gap in the silicide layer. A second gap in the silicide layer is created by self-alignment close to the first gap. Self-organization during annealing of the sample leads to the formation of a silicide wire with low energy (111) facets (figure 20). These wires have a width of 40 nm which is well beyond the resolution of the optical lithography used (1 μm).

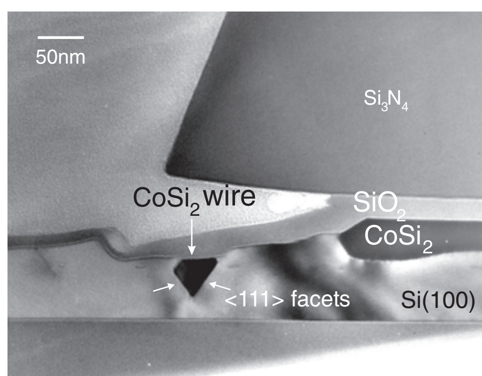

Figure 20. A cross section of a $CoSi_2$ wire with a diameter of 40 nm. The triangular form arises due to self-organization [20].

9. Conclusion

To fabricate semiconductor devices of dimensions beyond the limits of lithography alternative methods have to be explored. Self-organized growth of semiconductor nanostructures is one of these alternative approaches. Several examples of the formation of self-organized nanostructures have been presented, including the controlled formation of different kinds of two-dimensional Si/Ge nanostructure, such as nanowires, nanowire superlattices and nanorings. The nanostructures grown have a width down to 3.5 nm and a sub-nanometre thickness (0.3 nm), corresponding to a cross section consisting of only ∼21 atoms. STM operation at high temperatures during growth opens the possibility to observe the growth history of single growth features in real time. In particular, self-organization at prestructured substrates and the use of hybrid methods are most promising for connecting nanostructures formed by self-organization to mesoscopic lithographically patterned structures in order to provide electric contacts to the nanostructures.

References

[1] Eigler D M and Schweizer E K 1990 *Science* **344** 524
[2] Voigtländer B 2001 *Surf. Sci. Rep.* **43** 127
[3] Andersohn L, Berke Th, Köhler U and Voigtländer B 1996 *J. Vac. Sci. Technol.* A **14** 312
[4] Venables J A 1994 *Surf. Sci.* **299/300** 798
[5] Voigtländer B and Zinner A 1993 *Appl. Phys. Lett.* **63** 3055
[6] Voigtländer B, Zinner A and Weber Th 1996 *Rev. Sci. Instrum.* **67** 2568
[7] Voigtländer B and Weber Th 1996 *Phys. Rev. Lett.* **77** 3861
[8] Shimada W and Tochihara H 1994 *Surf. Sci.* **311** 107
[9] Voigtländer B, Kästner M and Smilauer P 1998 *Phys. Rev. Lett.* **81** 858
[10] Mo Y W, Savage D E, Schwartzentruber B S and Lagally M G 1990 *Phys. Rev. Lett.* **65** 1020
[11] Chen K M, Jesson D E, Pennycook S J, Thundat T and Warmack R J 1996 *Mater. Res. Soc. Symp. Proc.* **399** 271
[12] Kästner M and Voigtländer B 1999 *Phys. Rev. Lett.* **82** 2745
[13] Jesson D E, Voigtländer B and Kästner M 2000 *Phys. Rev. Lett.* **84** 330
[14] Liu F, Li A H and Lagally M G 2001 *Phys. Rev. Lett.* **87** 126103
[15] Voigtländer B and Zinner A 1996 *Surf. Sci. Lett.* **351** L233
[16] Voigtländer B, Kawamura M, Paul N and Cherepanov V 2003 *Phys. Rev. Lett.* **90** 096102
[17] Shiryaev S Y, Jensen F, Lundsgaard Hansen J, Wulff Petersen J and Nylandsted Larsen A 1997 *Phys. Rev. Lett.* **78** 503
[18] Kim E S, Usami N and Shiraki Y 1998 *Appl. Phys. Lett.* **72** 1617
[19] Vescan L and Stoica T 2002 *J. Appl. Phys.* **91** 10119
[20] Kluth P, Zhao Q T, Winnerl S, Lenk S and Mantl S 2001 *Appl. Phys. Lett.* **79** 824